

# Transformation dynamics of Ni clusters into NiO rings under electron beam irradiation



Daniel Knez<sup>a,b,\*</sup>, Philipp Thaler<sup>c</sup>, Alexander Volk<sup>c</sup>, Gerald Kothleitner<sup>a,b</sup>, Wolfgang E. Ernst<sup>c</sup>, Ferdinand Hofer<sup>a,b</sup>

<sup>a</sup> Institute of Electron Microscopy and Nanoanalysis, Graz University of Technology, Steyrergasse 17, 8010 Graz, Austria

<sup>b</sup> Graz Centre for Electron Microscopy, Steyrergasse 17, 8010 Graz, Austria

<sup>c</sup> Institute of Experimental Physics, Graz University of Technology, Petersgasse 16, 8010 Graz, Austria

## ARTICLE INFO

### Keywords:

Electron beam induced oxidation

NiO rings

Ni clusters

Kirkendall effect

Cabrera-Mott oxidation

Sample damage

## ABSTRACT

We report the transformation of nickel clusters into NiO rings by an electron beam induced nanoscale Kirkendall effect. High-purity nickel clusters consisting of a few thousand atoms have been used as precursors and were synthesized with the superfluid helium droplet technique. Aberration-corrected, analytical scanning transmission electron microscopy was applied to oxidise and simultaneously analyse the nanostructures. The transient dynamics of the oxidation could be documented by time lapse series using high-angle annular dark-field imaging and electron energy-loss spectroscopy. A two-step Cabrera-Mott oxidation mechanism was identified. It was found that water adsorbed adjacent to the clusters acts as oxygen source for the electron beam induced oxidation. The size-dependent oxidation rate was estimated by quantitative EELS measurements combined with molecular dynamics simulations. Our findings could serve to better control sample changes during examination in an electron microscope, and might provide a methodology to generate other metal oxide nanostructures.

## 1. Introduction

In recent years interest in metal and metal oxide nanostructures increased by virtue of their outstanding physical properties. This is particularly true for hybrid nanostructures with complementary magnetic or electric properties like in Ni/NiO, combining ferromagnetic/antiferromagnetic and conducting/dielectric characteristics [1–7]. The overcoming of the superparamagnetic limit by an antiferromagnetic environment, or strong optical nonlinearities in nanometer sized metal-dielectric composites have been reported for instance [8,9].

Consequently, the control of morphology, chemistry and oxidation behaviour of these structures is paramount for their application in emerging technologies, such as memristors, heterogeneous photocatalysis, energy storage, contrast agents in magnetic resonance imaging, magnetic data storage, sensors, and spintronics [10,2–6,8].

The oxidation kinetics of such metallic nanostructures is ruled by the nanoscale Kirkendall effect (NKE), which generally denotes void formation due to diffusivity differences at solid interfaces [11–17]. Usually the NKE is thermally activated, but the activation energy for the oxidation can also be provided by high-energy electrons, enabling localized triggering of the process even at non-elevated temperatures.

This effect is therefore important for nanofabrication techniques based on electron irradiation. Although electron beam induced oxidation was studied for a few medium and large sized nanostructures at different levels, the oxidation dynamics and the driving mechanisms for small Ni/NiO structures remain unexplored [18–21].

Here, we report and discuss the creation of single crystalline NiO ring structures consisting of less than 3000 nickel atoms (Fig. 1). The use of a focused electron beam, such as in an aberration corrected scanning transmission electron microscope (STEM), allows the local initialisation of a chemical reaction leading to interesting nanostructures regarding their chemistry, size and morphology. During the whole oxidation process, from a thin initial layer to full-oxidation, the transient evolution of the structure was observed in real-time via atomically resolved high-angle annular dark-field (HAADF) imaging, whereas the elemental distribution was studied with electron energy loss spectroscopy (EELS), being particularly sensitive for light elements.

In contrast to previous work, we started from supported Ni clusters grown inside superfluid He-droplets [22,23]. This technique allows the synthesis of high-purity clusters in ultra-high vacuum (UHV) conditions without templates or stabilizers, providing an ideal basis for

\* Corresponding author at: Institute of Electron Microscopy and Nanoanalysis, Graz University of Technology, Steyrergasse 17, 8010 Graz, Austria.

E-mail address: [daniel.knez@felmi-zfe.at](mailto:daniel.knez@felmi-zfe.at) (D. Knez).

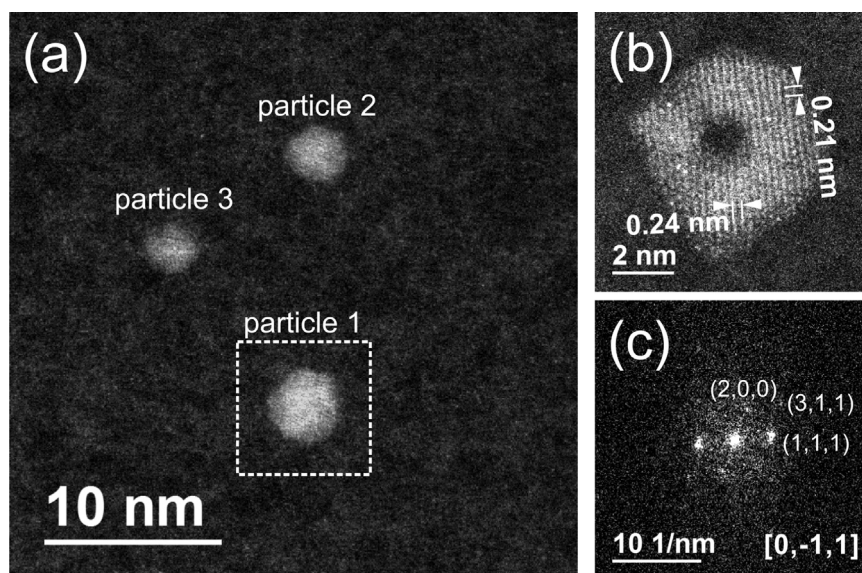


**Fig. 1.** (a) HAADF overview image of three clusters on amorphous carbon before oxidation. (b) Enlarged image of particle 1 after full transformation into a single crystalline NiO ring. (c) corresponding FFT from (b).

studying oxidation mechanisms without the influence of organic contamination. Such contaminants would otherwise lead to the formation of carbonaceous deposits in electron illuminated sample areas, which would disturb the oxidation kinetics and hence render the process difficult to control [19]. The formation of ring structures reported here would also be inhibited due to the stabilizing effect of carbon deposits on the clusters [24].

## 2. Material and methods

### 2.1. Cluster synthesis

Nickel clusters were grown inside superfluid He droplets with a mean diameter of 90 nm, consisting of about  $10^7$   $^4\text{He}$  atoms. To this end, pressurized (20 bar) high purity helium (99.9999%) is expanded through a cooled (8 K) nozzle (diameter  $\approx 5\ \mu\text{m}$ ) into vacuum. During the expansion, droplets are formed, whose final temperature is  $\approx 0.4\ \text{K}$  due to evaporative cooling [25]. The droplet beam is shaped by a skimmer and enters a second vacuum chamber housing the doping facilities. This is where Ni (99.998%) is thermally evaporated and the droplet beam is guided through the Ni-vapour. Atoms colliding with helium droplets are cooled to droplet temperature and aggregate in the centre of the droplet. Finally, the beam is terminated on a TEM-grid located in a third chamber. Upon collision with the substrate, the helium cushions the impact of the transported cluster and evaporates, leaving the bare cluster adsorbed on the surface [26]. The base pressures in all chambers are sufficiently low, so that no other atoms than Ni are picked up by the droplets, and deposition and storage of the samples in the last chamber take place under UHV conditions ( $p < 10^{-7}\ \text{Pa}$ ). A schematic representation of the synthesis apparatus is given in Fig. S1, Supporting Information.

### 2.2. Substrates

Clusters are deposited directly on commercial TEM substrates, such as amorphous carbon and graphene. Substrates covered by amorphous carbon (film thickness  $< 3\ \text{nm}$ ) and backed by a holey carbon support film on a 300 mesh gold grid (Ted Pella, Inc., Prod. No. 01824G) have been used. Suspended monolayer graphene on Quantifoil R2/4 holey carbon gold grids (from Graphenea Inc.) were used as graphene support. To eliminate contamination, graphene grids were baked at  $200\ ^\circ\text{C}$  in contact to active coal for 1 h before placed into the synthesis

facility [27]. After mounting in the deposition chamber, all substrates were baked for several hours at  $200\ ^\circ\text{C}$  under UHV conditions before cluster deposition. Although an evacuated vessel was used for the transfer from the synthesis facility to the microscope vacuum, the samples had to be exposed shortly ( $< 5\ \text{min}$ ) to ambient conditions.

### 2.3. Analysis

The experiments were performed using a probe-corrected FEI Titan<sup>3</sup> G2 60-300 STEM equipped with a Gatan Quantum energy filter for EELS. The microscope was operated either at 60 kV or 300 kV. Acquisition and evaluation of all data was carried out using Gatan DigitalMicrograph (GMS, version 2.31.764). Particle sizes in the HAADF image series were determined within MATLAB (version R2012b). As part of this procedure, each image was blurred using a  $3\times 3$  spatial averaging filter to reduce contrast variations introduced by the crystallinity of the clusters. Then a threshold based particle detection algorithm based on Otsu's method was applied (as implemented in the MATLAB image processing toolbox) [28]. The determined contours were used to calculate the projected area and centre of mass of the clusters.

### 2.4. Simulation and cluster size determination

EEL spectrum image data was acquired for 68 clusters with diameters between 1.5 nm and 2.8 nm. The Ni  $L_{2,3}$  edge and the low-loss range were recorded simultaneously in Dual-EELS mode, yielding the number of Ni atoms in each cluster via EELS quantification. To this end, background removal in the EEL spectra was performed by pre-edge power-law fitting and quantification was done by using a Hartree-Slater cross-section model within GMS. The projected area of each cluster was obtained from an HAADF image, acquired before spectra acquisition. The dose was kept as low as possible to minimize beam damage effects. Due to the limited signal-to-noise ratio, the threshold for particle detection was set manually for each single image. The projected area  $A$  of each particle was then plotted as a function of the number of atoms  $N$  (Fig. 2c). This data set was compared to molecular dynamics simulations of supported clusters within the same size range from 200 to 1200 atoms and we found reasonable agreement. For each cluster size up to 3000 atoms, 5 simulation runs were performed and a power law function was fitted ( $A \propto N^{\frac{2}{3}}$  for a spherical symmetry). The obtained fitting function was then used to extract volumetric informa-

Download English Version:

<https://daneshyari.com/en/article/5466855>

Download Persian Version:

<https://daneshyari.com/article/5466855>

[Daneshyari.com](https://daneshyari.com)